RAA 2021 Vol. **21** No. **4**, 100(6pp) doi: 10.1088/1674-4527/21/4/100

http://www.raa-journal.org *http://iopscience.iop.org/raa*

***R**esearch in*
***A**stronomy and*
***A**strophysics*

HI detection of J030417.78+002827.4 by the Five-hundred-meter Aperture Spherical Radio Telescope

Nai-Ping Yu[1,2], Lei Qian[1,2], Chuan-Peng Zhang[1,2], Peng Jiang[1,2], Jin-Long Xu[1,2] and Jun-Jie Wang[1]

[1] National Astronomical Observatories, Chinese Academy of Sciences, Beijing 100101, China; *npyu@bao.ac.cn*
[2] CAS Key Laboratory of FAST, National Astronomical Observatories, Chinese Academy of Sciences, Beijing 100101, China

Received 2020 September 18; accepted 2020 November 16

Abstract We present the first HI 21 cm spectroscopy detection of J030417.78+002827.4, which is an active galactic nucleus (AGN) with an intermediate-mass black hole (IMBH) in the center. The observations were carried out with the Five-hundred-meter Aperture Spherical Radio Telescope (FAST) last year. We relied on the ON-OFF observing approach with the 19-beam receiver covering 1.05 – 1.45 GHz. Within a total integration time of about 20 min, the root mean square (RMS) of our data reaches 1.2 mJy beam^{-1}, at a velocity resolution of 1.6 km s^{-1}. Radio frequency interference (RFI) is checked and excluded during the data analysis. The detected HI spectroscopy shows a dual-horned profile with a line width of 223.5 km s^{-1}, indicating gas rotation around this AGN. The redshift of this galaxy derived from our HI observation is 0.0447. We calculate the atomic gas mass by the integrated flux of the HI emission line. The total gas mass in this galaxy is estimated to be $1.8 \times 10^{10}\ M_{\odot}$. We find the fraction of gas-to-stellar mass ratio in J030417.78+002827.4 is more than 50%. This ratio is much higher than the typical value found in other AGNs with supermassive black holes (SMBHs), and is comparable to some star-forming galaxies recently observed by FAST.

Key words: galaxies: ISM — radio line: profiles

1 INTRODUCTION

As the most abundant element in the Universe, hydrogen has fundamental importance in the study of galaxies (e.g., Payne 1925; Yun et al. 1994). In visible wavelengths, cold interstellar gas hardly emits radiation. However, cold neutral hydrogen gas ($\sim$ 120 K) in gas rich galaxies could be easily detected through radio emission of 21 cm, which is known as the spin-flip transition (e.g., Haynes & Giovanelli 1984; Robinson et al. 2019).

The HI 21 cm emission line provides useful information on the host galaxy. Firstly, by the Doppler-shifted recessional velocities of HI, we can measure the redshift of galaxies. The value of galaxy redshift derived through this way is more reliable than that derived by optical emission lines such as [O III] (e.g., Mirabel & Wilson 1984). Secondly, in inclined disk galaxies, the observed HI emission lines are examined for the appearance of asymmetric profiles. This leads to the possibility of probing possible gas rotations and/or gas inflows of disk galaxies (e.g., Epstein 1964; Deg et al. 2020). Thirdly, we can rely on the optically thin emission of HI 21 cm spectroscopy to estimate the total atomic gas masses of galaxies, as atomic hydrogen is the dominant gas phase in disk galaxies (e.g., Roberts 1962). Given the fundamental importance of the HI component, many studies have been carried out to probe neutral atomic gas at low redshift (e.g., Heckman et al. 1978; Giovanelli et al. 2005).

Intermediate-mass black holes (IMBHs) are important for studies of black hole (BH) formation and growth, galaxy formation and evolution. (Following Green & Ho 2007, we here refer to BHs with masses less than 2×10^6 $M_{\odot}$ as IMBHs.) They are predicted to be an integral phase of supermassive black hole (SMBH) formation. However, the known population of IMBHs remains small and there are only a few HI detections in their host galaxies (e.g., Musaeva et al. 2015; Robinson et al. 2019). In order to build a homogeneous IMBH sample, Dong et al. (2012) conducted a systematic search for IMBHs in active galactic nuclei (AGNs) with broad H_{α} emission lines. They found a sample of 309 type 1 AGNs with BH masses in the range of 8×10^4 to 2×10^6 $M_{\odot}$. With the aim to

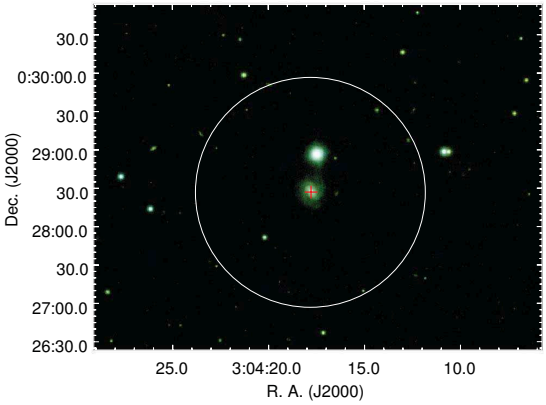

Fig. 1 A three color image of J030417.78+002827.4 utilizing the g, i, and z band filters from the Panoramic Survey Telescope and Rapid Response System (Pan-STARRS; Chambers et al. 2016). The *red cross* marks the center of this galaxy, and the *large white circle* indicates the beam size of FAST. There are no other known galaxies within this circle from the SDSS catalog.

probe the large-scale gas environment around these AGNs, we selected 14 sources from this sample and observed them with the Five-hundred-meter Aperture Spherical Radio Telescope (FAST) in 2019. Among these sources, we found J030417.78+002827.4 shows distinct HI line emission. (An optical image of this source is displayed in Fig. 1.) We introduce our FAST observations and data calibrations in Section 2, results and analysis in Section 3, and finally we summarize in Section 4.

2 FAST OBSERVATIONS AND CALIBRATIONS

With a diameter of 500 m, FAST is currently the largest single-dish telescope in the world. It passed its national acceptance on 2020 January 11. The extraordinary capability of the FAST 19-beam receiver has been confirmed to satisfy expectation by spectral HI observations towards various sources (e.g., Jiang et al. 2020; Cheng et al. 2020).

In 2019, we performed FAST HI observations of 14 galaxies in L-band with the 19-beam receiver (Proposal ID: 3056; PI: Lei Qian). Near the frequency of 1.4 GHz, the half-power beamwidth (HPBW) of each beam is about 2.9 arcmin diameter, separated by 5.8 arcmin from each other (Jiang et al. 2020). The observations were carried out in the tracking mode. Each source was observed for 20 minutes. During the first 10 minutes, we pointed the central Beam (M01) to the center of our sources (ON-target). During the next 10 minutes, we directed Beam 16 (M16) to the center of the sources instead. The OFF-target pointing positions were chosen at 5.8 arcmin distance, with no known galaxies in the field of view with a similar redshift (from the SDSS catalog) to our sources.

2.1 General Calibrations

A noise injection system was used for FAST signal calibrations. When the noise diode was switched on, a noise with known temperature was injected into the receiver. It was switched on and off repeatedly with a period of 1.00663296 s during the whole observation (an example is displayed in Fig. 2). Thus, for each source of ON-target, we recorded about 600 spectra with noise on (${Power_{\rm ON}}^{\rm cal\ on}$) and 600 spectra with noise off (${Power_{\rm ON}}^{\rm cal\ off}$). The antenna temperature of ON-target (${T_{\rm ON}}^{\rm cal\ off}$) could be calculated through

$$T_{\rm ON}^{\rm cal\ off} = T_{\rm noise} \times \frac{Power_{\rm ON}^{\rm cal\ off}}{Power_{\rm ON}^{\rm cal\ on} - Power_{\rm ON}^{\rm cal\ off}}\,, \quad (1)$$

where $T_{\rm noise}$ is the known injected noise temperature. The antenna temperature of OFF-target (${T_{\rm OFF}}^{\rm cal\ off}$) could also be calculated through this way. The antenna temperature (T_a) of each source could be calculated by $T_a = {T_{\rm ON}}^{\rm cal\ off} - {T_{\rm OFF}}^{\rm cal\ off}$. The derived spectra of ${T_{\rm ON}}^{\rm cal\ off}$, ${T_{\rm OFF}}^{\rm cal\ off}$ and T_a are plotted in Figure 3.

Flux density (in the unit of Jy) of a point source can be converted from its antenna temperature by dividing by the gain value. According to table 5 in Jiang et al. (2020), we adopted the gain values of 16.0 K Jy^{-1} and 13.3 K Jy^{-1} for M01 and M16, respectively. The final averaged HI spectrum is depicted in Figure 4. The root mean square (RMS) is about 1.2 mJy beam^{-1}, with a velocity resolution of 1.6 km s^{-1}.

2.2 Radio Frequency Interference

The above describes general calibrations of our FAST data. However, in the data reduction of each individual source, we should be careful of radio frequency interference (RFI). In Figure 2, it can be noticed that RFI has always been ubiquitous through the raw FAST data. In order to reduce the influence of RFI, we divided our data into batches of 10 s (5 s with noise on and 5 s with noise off), and then we checked the batches one by one by eye. In the data of J030417.78+002827.4, we found distinct RFI in the time range of 140 s to 160 s, 180 s to 220 s, and 480 s to 530 s (see Fig. 5). It can be noticed that RFI appears in one polarization. Data observed during these times are thus not involved in the analysis.

3 RESULTS

The final HI spectrum of J030417.78+002827.4 is presented in Figure 4. It displays a dual-horned profile, indicating

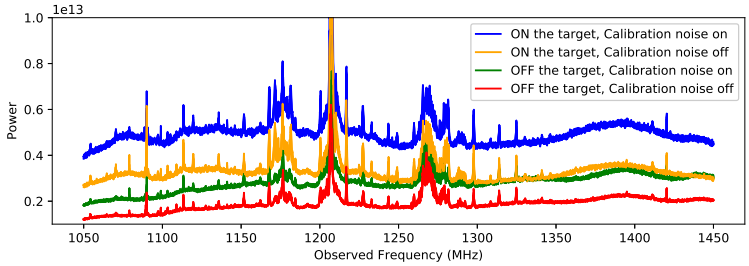

Fig. 2 The four cases of split raw spectra of our data in the first 10 s: ON-target with calibration noise on ($Power_{ON}^{calon}$), ON-target with calibration noise off ($Power_{ON}^{caloff}$), OFF-target with calibration noise on ($Power_{OFF}^{calon}$) and OFF-target with calibration noise off ($Power_{OFF}^{caloff}$).

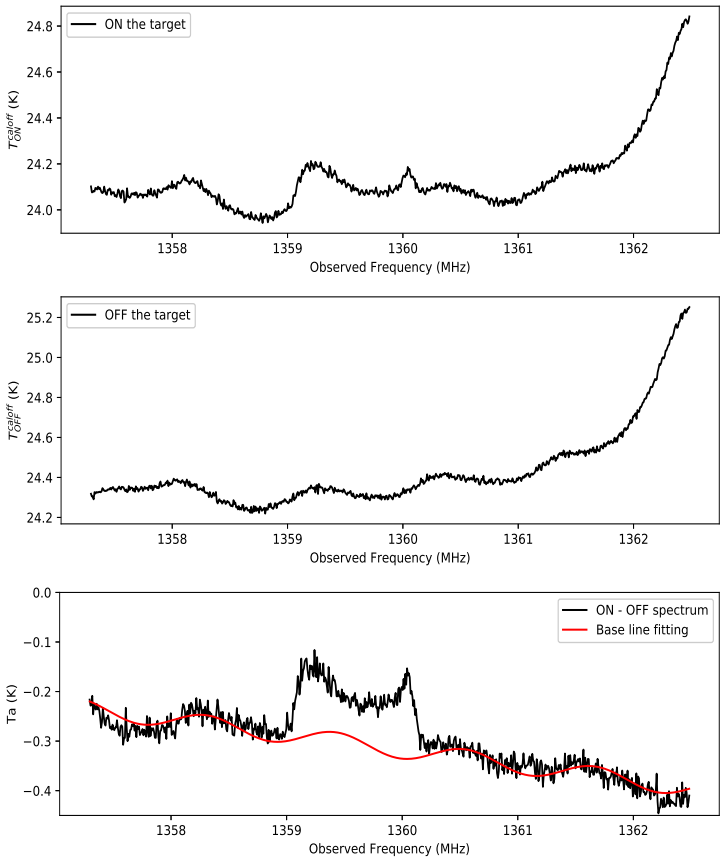

Fig. 3 Average spectra of ON the target (*top*), OFF the target (*middle*) and the antenna temperature (*bottom*) of J030417.78+002827.4. In the bottom panel, we fit the baseline with the function $a \times \sin(kx + b) + mx + n$ to account for the standing wave.

gas rotation around this AGN. In order to measure its parameters such as emission-line width, center-line recessional velocity (V_R) and integrated flux, we utilized the BusyFit software developed by Westmeier et al. (2014). The fitting function has the form of

$$\begin{aligned} B(x) =& \frac{a}{4} \times (\mathrm{erf}[b_1\{w + x - x_e\}] + 1) \\ & \times (\mathrm{erf}[b_2\{w - x + x_e\}] + 1) \\ & \times (c|x - x_p|^n + 1), \end{aligned} \tag{2}$$

where x is the spectral axis (frequency or velocity), a is the amplitude of the whole function, b_1 and b_2 are two independent slopes of the HI line flanks, w is the half-width of the HI emission line, x_e and x_p are the offsets added in order to fit asymmetric profile shapes, and c is the amplitude scaling factor of the central trough which is fitted with a polynomial of degree n. Values of $c > 0$ suggest increasing amplitudes of the trough, while for $c = 0$ the trough will disappear. The two error functions, $\mathrm{erf}(x)$, fit the two sides of the HI profile.

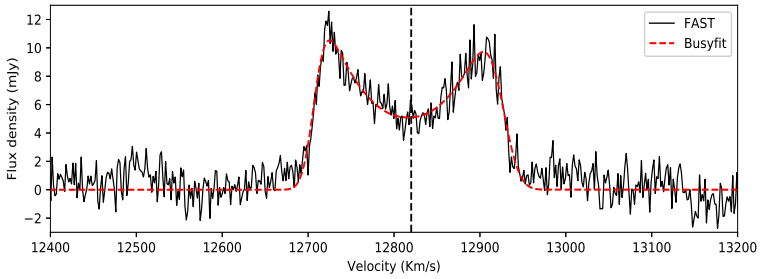

Fig. 4 HI emission line spectrum of J030417.78+002827.4 after calibration and baseline subtraction. The profile fitted by BusyFit software is traced in a *dashed red line*. The *dashed vertical line* indicates V_R derived from BusyFit.

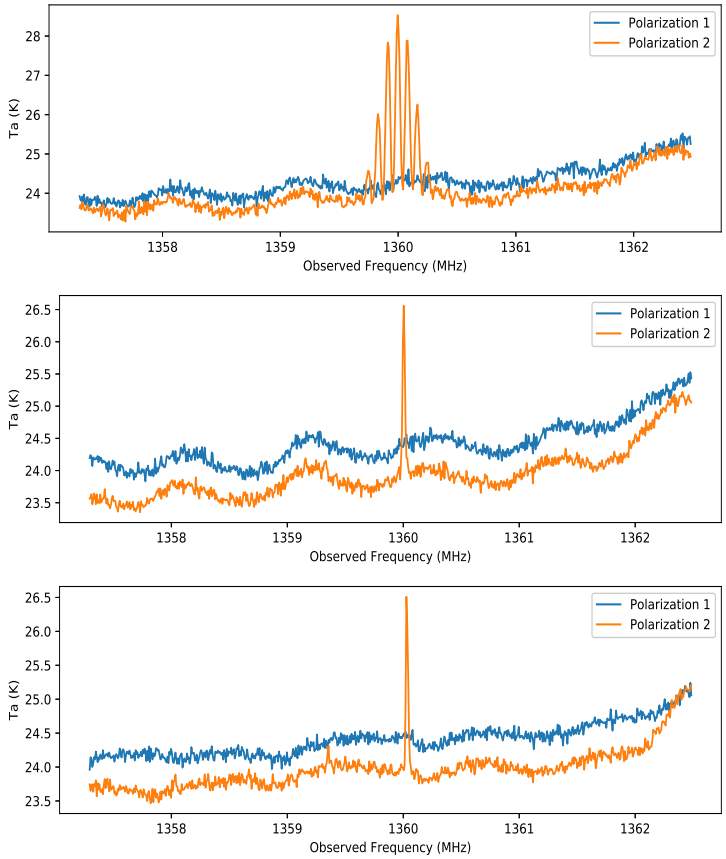

Fig. 5 RFI in the time range of 140 s to 160 s (*top*), 180 s to 220 s (*middle*), and 480 s to 530 s (*bottom*).

For well-defined profiles, BusyFit is able to automatically determine the best-fit parameters (e.g., Westmeier et al. 2014; Robinson et al. 2019). The best-fitting line is also shown in Figure 4. Through this method, we found the HI spectral line width of J030417.78+002827.4 is 223.5 $\pm$ 8.9 $\mathrm{km\ s^{-1}}$, with center-line recessional velocity of about 12820 $\pm$ 9 $\mathrm{km\ s^{-1}}$and the total integrated line flux is 1.6 $\pm$ 0.2 Jy $\mathrm{km\ s^{-1}}$.

Based on the HI line parameters derived above, we estimated the redshift of this galaxy to be 0.0447, which is nearly the same as its optical value ($z_{\mathrm{opt}} \sim 0.0445$) derived by Dong et al. (2012). If we adopt a ΛCDM cosmology of H_0 = 72 $\mathrm{km\ s^{-1}Mpc^{-1}}$ (Freedman et al. 2001), the distance of this galaxy could be estimated to be 178 $\pm$ 7 Mpc. (An uncertainty of 500 $\mathrm{km\ s^{-1}}$is adopted to account for peculiar velocities that may affect the distance derived from the redshift.) On the assumption that the HI emission is optically thin, we derive the HI gas mass following Giovanelli & Haynes (2015)

$$\frac{M_{\mathrm{HI}}}{M_{\odot}} = \frac{2.35 \times 10^5 D^2_{\mathrm{Mpc}}}{1+z} \int S(V) dv\,, \qquad (3)$$

where $S(V)$ is the flux density in the unit of Jy beam^{-1}. The total gas mass of a galaxy is then related to its HI gas mass through M_{GAS} = 1.4 M_{HI} (Cox 2000). The scale

factor of 1.4 accounts for the atomic helium gas mass in this galaxy assuming solar abundance. We then estimated the total gas mass of J030417.78+002827.4 to be $(1.8 \pm 0.2) \times 10^{10}\,M_{\odot}$.

Utilizing the SDSS photometry and the package MAGPHYS (da Cunha et al. 2008), Marleau et al. (2017) estimated the stellar mass of J030417.78+002827.4 to be $3.5 \times 10^{10}\,M_{\odot}$. We find the fraction of gas-to-stellar mass ratio ($M_{\rm HI}$ / $M_{\rm stars}$) is about 52%. This ratio is much higher than the typical value ($\sim 10\%$) ascertained in other AGNs with SMBHs in their centers (Robinson et al. 2019). Cheng et al. (2020) recently reported their FAST HI observations of three star-forming galaxies. We find the gas mass and gas-to-stellar mass ratio of our source are similar to their results. We thus suggest that there is a lot of gas for star formation in J030417.78+002827.4, even though more observations are still needed.

4 SUMMARY

We report the first HI 21 cm spectroscopy detection in J030417.78+002827.4 from the FAST observations. The detected HI spectroscopy exhibits a dual-horned profile, indicating gas rotation around this AGN. With the BusyFit software we derive the basic parameters of this spectrum. The width of our detected HI emission line is about $223.5\,{\rm km\,s^{-1}}$. The redshift of this galaxy is 0.0447. We calculate the atomic gas mass by the integrated flux of the HI emission line. The total gas mass is estimated to be $1.8 \times 10^{10}\,M_{\odot}$. We find the $M_{\rm HI}$ / $M_{\rm stars}$ ratio in J030417.78+002827.4 is 52%. This ratio is much higher than the typical value found in other AGNs with SMBHs, and is comparable to some star-forming galaxies recently observed by FAST. We thus suggest that there is a lot of gas for star formation in J030417.78+002827.4.

Acknowledgements We thank the anonymous referee for thorough and helpful comments and suggestions. This work has been supported by the Youth Innovation Promotion Association of Chinese Academy of Science (CAS), the National Natural Science Foundation of China (Grant Nos. 11703040 and 11933011), and also supported by the Open Project Program of the Key Laboratory of FAST, NAOC, Chinese Academy of Sciences. Lei Qian is supported by the National Natural Science Foundation of China (Grant No. U1631237) and the Youth Innovation Promotion Association of CAS (id.2018075). Chuan-Peng Zhang acknowledges supports from the Cultivation Project for FAST Scientific Payoff and Research Achievement of CAMS-CAS.

References

Chambers, K. C., Magnier, E. A., Metcalfe, N., et al. 2016, arXiv e-prints, arXiv:1612.05560
Cheng, C., Ibar, E., Du, W., et al. 2020, A&A, 638, L14
Cox, A. N. 2000, Allen's astrophysical quantities
Deg, N., Blyth, S. L., Hank, N., et al. 2020, MNRAS, 495, 1984
da Cunha, E., Charlot, S., & Elbaz, D. 2008, MNRAS, 388, 1595
Dong, X.-B., Ho, L. C., Yuan, W., et al. 2012, ApJ, 755, 167
Epstein, E. E. 1964, AJ, 69, 490
Freedman, W. L., Madore, B. F., Gibson, B. K., et al. 2001, ApJ, 553, 47
Giovanelli, R., & Haynes, M. P. 2015, A&A Rev., 24, 1
Giovanelli, R., Haynes, M. P., Kent, B. R., et al. 2005, AJ, 130, 2598
Greene, J. E., & Ho, L. C. 2007, ApJ, 670, 92
Greene, J. E., Strader, J., & Ho, L. L. C. 2020, ARA&A, in press (arXiv:1911.09678)
Haynes, M. P., & Giovanelli, R. 1984, AJ, 89, 758
Heckman, T. M., Balick, B., & Sullivan, W. T., I. 1978, ApJ, 224, 745
Jiang, P., Tang, N.-Y., Hou, L.-G., et al. 2020, RAA (Research in Astronomy and Astrophysics), 20, 064
Marleau, F. R., Clancy, D., Habas, R., &, Bianconi, M. 2017, A&A, 602, A28
Mirabel, I. F., & Wilson, A. S. 1984, ApJ, 277, 92
Musaeva, A., Koribalski, B. S., Farrell, S. A., et al. 2015, MNRAS, 447, 1951
Payne, C. H. 1925, Stellar Atmospheres; a Contribution to the Observational Study of High Temperature in the Reversing Layers of Stars, PhD thesis, RADCLIFFE COLLEGE
Roberts, M. S. 1962, AJ, 67, 437
Robinson, J. H., Bentz, M. C., Johnson, M. C., et al. 2019, ApJ, 880, 68
Westmeier, T., Jurek, R., Obreschkow, D., et al. 2014, MNRAS, 438, 1176
Yun, M. S., Ho, P. T. P., & Lo, K. Y. 1994, Nature, 372, 530